Neutron Stars in Supernova Remnants
ASP Conference Series, Vol. 9999, 2002
P. O. Slane and B. M. Gaensler, eds.

Chandra X-ray Spectroscopy of Kes 75, its Young Pulsar, and its Synchrotron Nebula

B. F. Collins, E. V. Gotthelf, and D. J. Helfand

Columbia Astrophysics Laboratory, 550 West 120th St, New York, NY 10027, USA

Abstract. We have observed the young Galactic supernova remnant Kes 75 with the Chandra X-ray Observatory. This object is one of an increasing number of examples of a shell-type remnant with a central extended radio core harboring a pulsar. Here we present a preliminary spatially resolved spectroscopic analysis of the Kes 75 system. We find that the spectrum of the pulsar is significantly harder than that of the wind nebula, and both of these components can be isolated from the diffuse thermal emission that seems to follow the same distribution as the extended radio shell. When we characterize the thermal emission with a model of an under-ionized plasma and non-solar elemental abundances, we require a significant diffuse high energy component, which we model as a power-law with a photon index similar to that of the synchrotron nebula.

1. Introduction

Kes 75 (also known as G29.7−0.3) is one example in our Galaxy of a young, shell-type remnant ($3.5'$ in diameter) with a central core ($30''$) whose observed properties suggest a synchrotron nebula similar to the Crab Nebula (Becker, Helfand & Szymkowiak 1983; Becker & Helfand 1984; Blanton & Helfand 1996). Observations by the Advanced Satellite for Cosmology and Astrophysics (*ASCA*) verified the existence of both thermal and non-thermal emission, but lacked the spatial resolution necessary to separate the components (Blanton & Helfand 1996). Monitoring with the Rossi X-Ray Timing Explorer led Gotthelf et al. (2000) to discover a 700 year old pulsar, PSR J1846−0258, located in the *ASCA* data within the Crab-like core. Expanding on the previous work, we discover a significant spectral difference between the pulsar and the surrounding wind nebula. Using a non-equilibrium ionization model we find different temperature and heavy-metal abundances in separate regions of the shell, as well as evidence of non-thermal emission throughout.

2. Observations

We report here on an observation of the supernova remnant Kes 75 obtained on $10 - 11$ Oct 2000 with the Chandra X-ray Observatory (Weisskopf, O'Dell, & van Speybroeck 1996). Photons were collected using the Advanced CCD

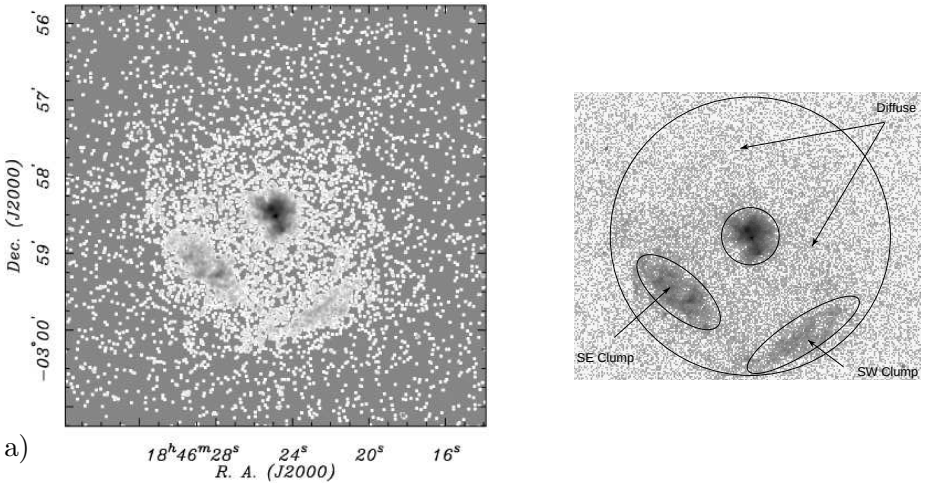

Figure 1. a) Chandra X-ray image of Kes 75. Logarithmic scaling is used to highlight the smooth, fainter emission and the overall circular symmetry. The pulsar is indicated by the central bright spot surrounded by the bright wind nebula. b) Kes 75 with spectral extraction regions indicated.

Imaging Spectrometer (ACIS), with the target placed on S3 chip. This back-side illuminated CCD is sensitive to photons in the $\sim 0.2-10$ keV energy range with a spectral resolution of $E/\Delta E \sim 10$ at 1 keV and an on-axis angular resolution of $\sim 0\farcs5$ at 1 keV. We processed Level 1 data with the charge transfer inefficiency reduction algorithms created by Townsley et al. (2000), and then chose the *ASCA*-like [0, 2, 3, 4, 6] grade set from the resulting event list for our analysis. We created a lightcurve from the non-source data on the ACIS-S3 chip to select Good-Time Intervals free of unusually high background activity. After all processing, we had obtained 34 ks of exposure time. A high level of absorption toward the source blocked most photons with energy ≤ 1, so all models were fit on the energy range of $1-7$ keV. All spectra were grouped to contain a minimum of 20 counts bin^{-1}, and all errors are quoted to the 1-σ confidence range.

3. Results

We centered a small circular aperture with an $\sim 2''$ radius on PSR J1846−0258, and a larger elliptical region to contain the entire pulsar wind nebula. The count rate of the pulsar itself produces noticeable CCD pile-up effects and renders background contamination insignificant. For the wind nebula and its subdivisions, we subtracted background spectra from a patch of smooth emission just southwest of the core, but within the shell of the supernova remnant; the count rate for the nebula is insufficient to cause concern over pile-up. Because all of the photons from the central source fall onto a relatively small area of the CCD, the instrumental response for all of the regions can be described sufficiently with the ACIS-S3 RMF provided with the CTI reduction software and a single point

source mirror response (ARF) created for PSR J1846−0258 with the standard CIAO tools, but incorporating the supplied CTI-adjusted QEU file.

In the center of the remnant, the pulsar and its wind nebula are both clearly resolved. Outside of the bright central nebula, an expanse of faint diffuse emission is visible, with two brightened features along the southern edge. We encompass all of the diffuse shell with a 200″ wide circular aperture, centered on PSR J1846−0258. From this region we exclude the elliptical region of the pulsar and its wind nebula. We also drew an ellipse around each of the 'clumps' in the south, to analyze them separately, and exclude them from the fainter emission. For the background subtraction of all regions, we used an off-source area of the S3 chip, to the northwest of Kes 75. Using the point-like ARF no longer sufficed for our extended faint source. Instead, we used software created by A. Vikhlinin to weight each 32×32 pixel response region by X-ray flux, and average them together over the whole extraction aperture, again incorporating the new QEU file. We continued to use the supplied CTI-adjusted RMF.

3.1. PSR J1846−0258 and the Synchrotron Nebula

To account for the phenomenon of CCD pile-up in our observation, we employed the `pileup` model included in XSPEC v11.1.0p. Since this model is still in the testing phase, we stress the preliminary nature of our result. We fit the spectrum with an absorbed power-law, which consistently produced better fits than blackbody or bremsstrahlung continua. The best fit parameters of the piled-up, absorbed power-law model are $\Gamma = 1.2 \pm 0.1$, and $N_H = 3.5 \pm 0.2 \times 10^{22}$ cm^{-2}, with a reduced $\chi^2_\nu = 0.86$ (58 dof). The best-fit column density seemed to border on agreement with the best-fit column density of the entire wind nebula ($3.95 \pm 0.07 \times 10^{22}$ cm^{-2}). Since it is not piled-up and is less affected by the possibly extreme environments immediately surrounding a pulsar, we decided this was a more reliable estimate, froze the parameter, and re-fit. The photon index increased to 1.5 ±0.1.

Compared to the pulsar, the central elliptical region shows a spectra just as devoid of emission lines that produces equally poor fits to thermal models. In terms of the power-law photon index, the nebula is unique ($\Gamma = 1.91 \pm 0.04$). Confidence contours of the column density and photon index for the entire wind nebula region demonstrate that the two regions are spectrally distinct.

3.2. The Thermal Shell

To analyze the emission from the shell of Kes 75, we followed two approaches. Using an arbitrary thermal bremsstrahlung continuum with three Gaussians to represent the most prominent emission lines, we aimed to reproduce the thermal components of a model fit to the *ASCA* observation by Blanton & Helfand (1996), and to compare the spectra from different parts of the shell. In the other case we chose models that more appropriately characterized emission from the ionized plasma of a supernova remnant.

Fitting the arbitrary bremsstrahlung and Gaussians model to the data extracted 15″ to 100″ from the pulsar, the positions of the three strongest spectral lines correspond to the ions Mg XI, Si XIII, and S XV, and are all consistent with their counterparts in the *ASCA* analysis. The plasma temperature and column density of the best-fit model, however, disagree drastically.

The spectra extracted from the bright clumps in the southern portion of the remnant, when compared the emission elsewhere in the shell, exhibit similar Mg XI, Si XIII, and S XV lines, and yield the same best-fit column density. The values of kT are much higher in the clumps than in the faint background, indicating only that their spectra are generally softer.

A single non-equilibrium ionization collisional plasma model (Borkowski et al. 2001) with interstellar absorption and varying abundances fit both the continuum and the emission lines of each spectra poorly. When we add a power-law component, however, the fits improve dramatically. We froze the column density at the value fit to the pulsar wind nebula, and fit each region twice, once varying the elemental abundances together in solar ratios, and once letting each element whose X-ray emission lies primarily within the energy range of our analysis vary independently. The results indicate different elemental ratios and ion densities for the different regions of the remnant. Additional in depth analyses of these models will be presented in a forthcoming paper.

4. Discussion

For the *ASCA* observation of Kes 75, it was not possible to extract only the spectrum of the central Crab-like component of the supernova remnant without the surrounding thermal part, only to fit a model to all the data that accounts for both of the components. Given this limitation, Blanton & Helfand (1996) characterized all the non-thermal emission of the object with a single power-law ($\Gamma = 2.0$). We can now resolve the core from the shell, and analyze their spectra individually. The clearly non-thermal spectrum of the central nebula exhibits a photon index consistent with the *ASCA* findings, yet if this were the sole source of non-thermal flux, our heuristic model of the shell portion should be just as consistent with the previous results. The lack of similarity between the two spectra indicates a significant amount of non-thermal flux from outside the central core of the remnant. This extra emission may account for the spectral inconsistencies between the line strengths and the thermal continuum.

Acknowledgments. This research is supported by CXC grant SAOGO0-1130X. E. V. G. is supported by NASA LTSA grant NAG5-22250.

References

Becker, R. H., Helfand, D. J. & Szymkowiak, A. E. 1983, ApJ, 268, 93

Becker, R. H. & Helfand, D. J. 1984, ApJ, 283, 154

Blanton, E. L. & Helfand, D. J. 1996, ApJ, 470, 961

Borkowski, K. J., Lyerly, W. J. & Reynolds, S. P 2001, ApJ, 548, 820

Gotthelf, E. V., Vasisht, G., Boylan-Kolchin, M. & Torii, K. 2000, ApJ, 542, L37

Townsley, L. K., Broos, P. S., Garmire, G. P., & Nousek, J.A. 2000, ApJ, 534, L139

Weisskopf, M. C., O'Dell, S. L., & van Speybroeck, L. P. 1996, Proc. SPIE, 2805, 2